Controlling chaos of a Bose-Einstein condensate loaded into a moving optical Fourier-synthesized lattice

R. Chacon, D. Bote, and R. Carretero-González

October 15, 2008

Computational Science &
Engineering Faculty and Students
Research Articles

Database Powered by the
Computational Science Research Center
Computing Group & Visualization Lab

COMPUTATIONAL SCIENCE & ENGINEERING

SAN DIEGO STATE UNIVERSITY

Computational Science Research Center
College of Sciences
5500 Campanile Drive
San Diego, CA 92182-1245
(619) 594-3430

Controlling chaos of a Bose-Einstein condensate loaded into a moving optical Fourier-synthesized lattice

R. Chacón,[1] D. Bote,[2] and R. Carretero-González[3],*

[1]*Departamento de Física Aplicada, Escuela de Ingenierías Industriales, Universidad de Extremadura, Apartado Postal 382, E-06071 Badajoz, Spain*

[2]*Departamento de Matemáticas, Escuela de Ingenierías Industriales, Universidad de Extremadura, Apartado Postal 382, E-06071 Badajoz, Spain*

[3]*Nonlinear Dynamical Systems Group,† Computational Science Research Center,‡ and Department of Mathematics and Statistics, San Diego State University, San Diego, California 92182-7720, USA*

We study the chaotic properties of steady-state traveling-wave solutions of the particle number density of a Bose-Einstein condensate with an attractive interatomic interaction loaded into a traveling optical lattice of variable shape. We demonstrate theoretically and numerically that chaotic traveling steady states can be reliably suppressed by *small* changes of the traveling optical lattice shape while keeping the remaining parameters constant. We find that the regularization route as the optical lattice shape is continuously varied is fairly rich, including crisis phenomena and period-doubling bifurcations. The conditions for a possible experimental realization of the control method are discussed.

I. INTRODUCTION

The combination of a Bose-Einstein condensate (BEC) (see, e.g., the reviews [1,2]) and an optical lattice provides a unique scenario for exploring new quantum phenomena and their classical manifestations. In particular, the presence of chaos in BECs has become a subject of great interest, partly because of its technological implications. As is well known, a cause of the quantum suppression of chaos is that the (classical) chaos generally appears in nonlinear systems while the corresponding quantum Schrödinger equations are linear [3]. The possible existence of (classical) chaos in BECs comes from the fact that the dynamics of dilute atomic BECs, close to zero temperature, can be well approximated by a *nonlinear* Schrödinger equation—the so-called Gross-Pitaevskii equation (GPE) [1,2,4,5]. Indeed, diverse manifestations of temporal [6,7], spatial [8,9], and spatiotemporal [10,11] chaos in BECs have been reported recently, including the process of BEC collapse [12,13] and open BECs [14]. It would therefore seem clear that a fundamental problem to address when considering applications of BECs is the prediction and control of chaos. A recent study in this respect, for example, showed the suppressive effects of dissipation and the velocity of a traveling optical lattice [11].

The aim of the present work is to show that the dissipative chaotic dynamics of a BEC loaded into a moving optical lattice exhibits great sensitivity to small changes of the lattice shape and can thus be reliably controlled by Fourier-synthesizing suitable lattice shapes. It is worth mentioning that this technique has been successfully used to control quantum transport of an atomic BEC [15]. Moving optical lattices [16–18] and dissipative effects [6,19,20] have also been studied recently.

*http://www.rohan.sdsu.edu/~rcarrete/

†http://nlds.sdsu.edu/

‡http://www.csrc.sdsu.edu/

II. ANALYTICAL TREATMENT

Let us consider the case of a quasi-one-dimensional (1D) BEC that is tightly confined in two transverse directions (the so-called cigar-shaped condensate) described by the following 1D GPE:

$$\hbar(i + \gamma)\frac{\partial \psi}{\partial t} = -\frac{\hbar^2}{2m_a}\frac{\partial^2 \psi}{\partial x^2} + g_0|\psi|^2\psi + V_0 \text{sn}^2(\kappa\xi; m)\psi, \quad (1)$$

where $V_0\text{sn}^2(\kappa\xi; m)$ is the periodic moving optical lattice; $\xi = x + \delta t/(2k)$ is the space-time variable with δ being the frequency difference between the two Fourier-synthesized counter-propagating laser beams and $k = 2\pi/\lambda$ the laser wave vector which determines the velocity of the traveling lattice as $v_L = \delta/(2k)$; m_a is the atomic mass; $g_0 = 4\pi\hbar^2 a/m_a$ characterizes the attractive ($a < 0$ being the s-wave scattering length) interatomic interaction strength; $\kappa = 2K(m)k/\pi$ with $K(m)$ being the complete elliptic integral of the first kind; $\text{sn}(\cdot; m)$ is the Jacobian sine elliptic function of parameter $m \in [0, 1]$; and $\hbar\gamma\partial\psi/\partial t$ is a dissipation term [20–23]. The static version of the elliptic optical lattice in Eq. (1) has been studied extensively [24–30].

For the sake of simplicity, we shall here concentrate only on the traveling-wave solutions of Eq. (1) in the form of a Bloch-like wave

$$\psi = \varphi(\xi)\exp[i(\alpha x + \beta t)], \quad (2)$$

where α and β are real constants to be determined. Note that this choice implies that the traveling wave $\varphi(\xi)$ has the same velocity as the elliptic optical lattice. After inserting Eq. (2) into Eq. (1) and normalizing the function φ by the factor $k^{3/2}$ and the variable ξ by the factor $2K(m)/\pi$, one straightforwardly obtains the ordinary differential equation
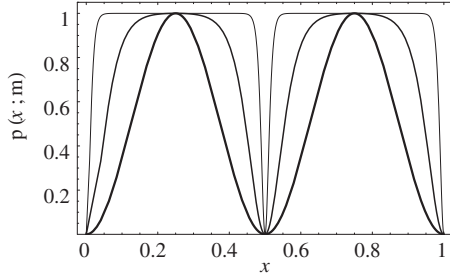
FIG. 1. Potential function $p(x;m)$ [cf. Eq. (5)] for $m=0$ (thick line), 0.995 (medium line), and $1-10^{-14}$ (thin line). The quantities plotted are dimensionless.

$$\frac{d^2\varphi}{d\zeta^2} + \gamma v \frac{d\varphi}{d\zeta} - (\widetilde{\beta} + \widetilde{\alpha}^2)\varphi - g|\varphi|^2\varphi$$

$$= -i\left((v + 2\widetilde{\alpha})\frac{d\varphi}{d\zeta} + \gamma\widetilde{\beta}\varphi\right) + \widetilde{V}_0 \mathrm{sn}^2[2K(m)\zeta/\pi;m]\varphi,$$

$$(3)$$

where $g=8\pi ak<0$ ($a<0$ since we are considering an attractive condensate), $\zeta=\kappa\xi$, $v=2m_a v_L/(\hbar k)$, $\widetilde{\alpha}=\alpha/k$, $\widetilde{\beta}=\hbar\beta/E_r$, and $\widetilde{V}_0=V_0/E_r$, with $E_r=\hbar^2 k^2/(2m_a)$ being the recoil energy.

Following Ref. [11], we express the complex function $\varphi(\zeta)$ in the form $\varphi(\zeta)=R(\zeta)e^{i\theta(\zeta)}$, and consider the simple situation where the phase $\theta(\zeta)$ has a linear dependence on the dimensionless space-time variable: $d\theta/d\zeta=-\widetilde{\beta}/v=-(v/2+\widetilde{\alpha})$ [36]. Note that R^2 represents the particle number density, whose chaotic dynamics we wish to suppress by reshaping the optical lattice potential. In this case, Eq. (3) reduces to a damped, parametrically and anharmonically driven, Duffing equation for the amplitude R:

$$\frac{d^2R}{d\zeta^2} - \left[\frac{v^2}{4} + \widetilde{V}_0 p\left(\frac{\zeta}{2\pi};m\right)\right]R - gR^3 = -\gamma v \frac{dR}{d\zeta}, \quad (4)$$

where we introduce the potential

$$p(x;m) \equiv \mathrm{sn}^2[4K(m)x;m]. \quad (5)$$

When $m=0$, then $p(\zeta/(2\pi);m)=\sin^2(\zeta)=\sin^2(k\xi)$, i.e., one recovers the previously studied case of a pure trigonometric optical lattice [11], while at the limiting value $m=1$ the elliptic optical lattice becomes constant except on a set of points of Lebesgue measure zero, i.e., one recovers a case with no moving periodic lattice where spatially chaotic steady states are no longer possible (see Fig. 1). Therefore, starting from a chaotic state at $m=0$, one would expect to observe a regularization of the traveling-wave steady states as $m\to 1$ while keeping the remaining parameters constant. To keep the analysis close to a possible experimental realization, we expand the elliptic optical lattice in the form

$$\mathrm{sn}^2(\zeta;m) = \sum_{j=1}^{\infty} b_{j-1} \sin^2\left(\frac{j\pi\zeta}{2K}\right), \quad (6)$$

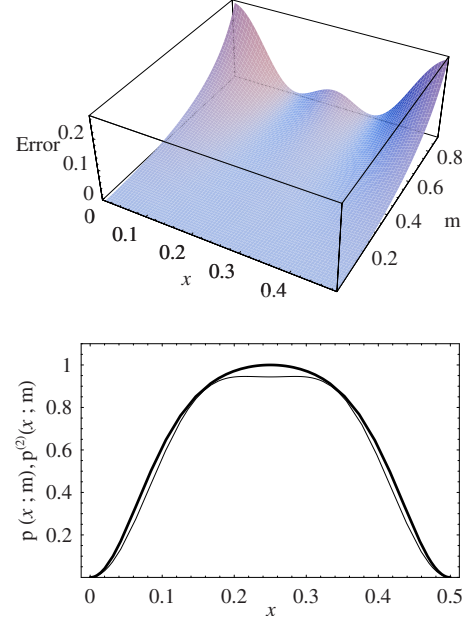where the first Fourier coefficients are approximately given by (see the Appendix for details)

FIG. 2. (Color online) Top panel: Relative error $[p(x;m)-p^{(2)}(x;m)]/p(x;m)$ with p as in Eq. (5) and $p^{(2)}$ corresponding to its two-term Fourier expansion as in Eq. (8). Shape parameter in the range $m \in [0, 0.9]$. Bottom panel: Functions $p(x;m=0.9)$ (thick line) and $p^{(2)}(x;m=0.9)$ (thin line), showing their proximity. The quantities plotted are dimensionless.

$$b_0 \simeq \frac{4\pi^2 q(1 - q + q^2 - q^3 + q^4)}{mK^2(1 - q - q^5 + q^6)},$$

$$b_1 \simeq \frac{8\pi^2 q^2(1 - q^4)}{mK^2(1 - q^3 - q^5 + q^8)},$$

$$b_2 \simeq \frac{4\pi^2 q^3}{mK^2(1 - q^3)^2}\left(1 + \frac{2(1 - q^3)^2}{(1 - q)(1 - q^5)}\right), \quad (7)$$

over the range $0 \leq m \leq 0.99$, and where $K=K(m)$, and $q=q(m)\equiv\exp[-\pi K(1-m)/K(m)]$ is the nome [31]. It will be useful to define the truncated Fourier expansion of order k for the elliptic optical lattice potential as

$$p^{(k)}(\zeta;m) \equiv \sum_{j=1}^{k} b_{j-1} \sin^2\left(\frac{j\pi\zeta}{2K}\right), \quad (8)$$

such that $p(\zeta/(2\pi);m)=\lim_{k\to\infty}p^{(k)}(\zeta;m)$.

To obtain an analytical estimate of the chaotic threshold in parameter space, let us assume in the following that the dissipation term and the optical lattice potential in Eq. (4) are small-amplitude perturbations of the underlying integrable two-well Duffing equation [32], i.e., they satisfy the Melnikov method (MM) requirements [32,33], and that, in the limiting case $m=0$, the perturbed Duffing equation (4) exhibits homoclinic chaos. Figure 2 depicts a comparison between the full potential (5) and its truncated Fourier expansion (8), when only the two first terms of the approximation for the elliptic parameter $m=0.9$ are retained. Figure 3 depicts the same comparison as in Fig. 2 but for a larger elliptic param-
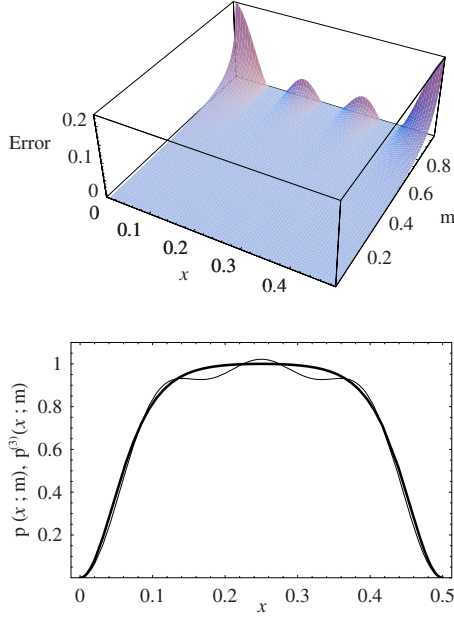
FIG. 3. (Color online) Top panel: Relative error $[p(x;m) - p^{(3)}(x;m)]/p(x;m)$, with p as in Eq. (5) and $p^{(3)}$ corresponding to its three-term Fourier expansion as in Eq. (8). Shape parameter in the range $m \in [0, 0.99]$. Bottom panel: Functions $p(\xi; m=0.99)$ (thick line) and $p^{(3)}(\xi; m=0.99)$, (thin line) showing their proximity. The quantities plotted are dimensionless.

eter $m=0.99$ when retaining three terms in the expansion (8). It is clear that using only the first two terms in the expansion is enough to accurately capture the main deviation of the Jacobian elliptic potential from a purely trigonometric one for values of the elliptic parameter up to $m \simeq 0.9$. Therefore, for the sake of simplicity, we only retain the two first terms of the expansion (6) and, after some simple algebraic manipulation, the application of the MM to Eqs. (4)–(7) yield the Melnikov function

$$M^{\pm}(\zeta) = \frac{\gamma v^4}{6g} + \frac{2\pi b_0 \widetilde{V}_0}{g} \operatorname{csch}\left(\frac{2\pi}{v}\right)\sin(2\zeta)$$
$$+ \frac{8\pi b_1 \widetilde{V}_0}{g} \operatorname{csch}\left(\frac{4\pi}{v}\right)\sin(4\zeta), \qquad (9)$$

where the plus (minus) sign corresponds to the right (left) homoclinic orbit of the unperturbed Duffing equation. Since $b_0(m=0)=1$, $b_1(m=0)=0$ [cf. Eq. (7)], the hypothesis of homoclinic chaos for a single-humped (pure) trigonometric optical lattice ($m=0$) implies that $2\pi b_0 \widetilde{V}_0 \operatorname{csch}(2\pi/v) > \gamma v^4/6$, which is a necessary condition for $M^{\pm}(\zeta)$ to present simple zeros at $m=0$. Thus, to analyze the suppressive effect of an elliptic optical lattice ($m>0$) we shall consider in the following the normalized Melnikov function

$$M_n^{\pm}(\zeta) = 1 + \beta_0 \sin(2\zeta) + \beta_0(b_0-1)\sin(2\zeta) + \chi\beta_0 b_1 \sin(4\zeta), \qquad (10)$$

where

$$M_n^{\pm}(\zeta) \equiv \frac{M^{\pm}(\zeta)}{\gamma v^4/(6g)},$$

$$\beta_0 \equiv \frac{12\pi\widetilde{V}_0 \operatorname{csch}(2\pi/v)}{\gamma v^4},$$

$$\chi \equiv \frac{4 \sinh(2\pi/v)}{\sinh(4\pi/v)}. \qquad (11)$$

Next, we study the appearance of simple zeros of $M_n^{\pm}(\zeta)$ with the constraint $\beta_0 > 1$ (i.e., there exists homoclinic chaos at $m=0$) by considering the zeros of the quartic polynomial in z which arises from Eq. (10) after the substitution $z = \sin(2\zeta)$. Solving this quartic equation, one straightforwardly obtains that a necessary condition for $M_n^{\pm}(\zeta)$ [and hence for $M^{\pm}(\zeta)$] to present simple zeros is

$$\beta_0^2[144\chi^2 b_0^2 b_1^2 + 1152\chi^4 b_1^4 + 2(b_0^2 - 4\chi^2 b_1^2)^2]^2$$
$$\leq 4[48\chi^2 b_1^2 + \beta_0^2(b_0^2 - 4\chi^2 b_1^2)^2]^3, \qquad (12)$$

where the equality provides the boundary function in the parameter space, and hence one obtains the chaotic threshold function $U(m,v)$ such that $\widetilde{V}_0/\gamma \geq U(m,v)$ provides a necessary condition for the perturbed Duffing equations (4)–(7) to exhibit homoclinic chaos [34]. Recalling that the Melnikov function (9) is approximately valid over the range $0 \leq m \lesssim 0.9$ and that $b_1 \ll b_0$ over this range [cf. Eq. (7)], one can drop the terms proportional to any power of b_1 in Eq. (12) to finally obtain an approximate necessary condition for the perturbed Duffing equations (4)–(7) to exhibit homoclinic chaos:

$$\frac{\widetilde{V}_0}{\gamma} \geq \widetilde{U}(m,v) \equiv \frac{\widetilde{U}_0(m=0,v)}{b_0(m)}, \qquad (13)$$

where

$$\widetilde{U}_0(m=0,v) \equiv \frac{v^4 \sinh(2\pi/v)}{12\pi} \qquad (14)$$

is the chaotic threshold function associated with a pure trigonometric optical lattice ($m=0$) [11].

Remarkably, the simplicity of condition (13) does not imply, however, a significant loss of accuracy with respect to the condition $\widetilde{V}_0/\gamma \geq U(m,v)$. Indeed, Fig. 4 indicates that the differences between the chaotic threshold functions $\widetilde{U}$ and U are noticeable only for values of the shape parameter very close to 1. The top panel of Fig. 5 shows a plot of the dimensionless function $\widetilde{U}(m,v)$. One sees that $\widetilde{U}(m=\text{const}, v)$ presents a single minimum as a function of the dimensionless lattice velocity (see, Fig. 5, bottom panel), while $\widetilde{U}(m, v=\text{const})$ presents a monotonically *increasing* behavior as a function of the shape parameter (see Fig. 5, middle panel), as expected. Therefore, if one considers fixing the parameters (V_0, γ, k, v_L, and hence v) for the particle number density of the BEC to exhibit chaos at $m=0$, then as m is increased a window of regular dynamics will appear, provided the initial chaotic state is sufficiently near the cha-
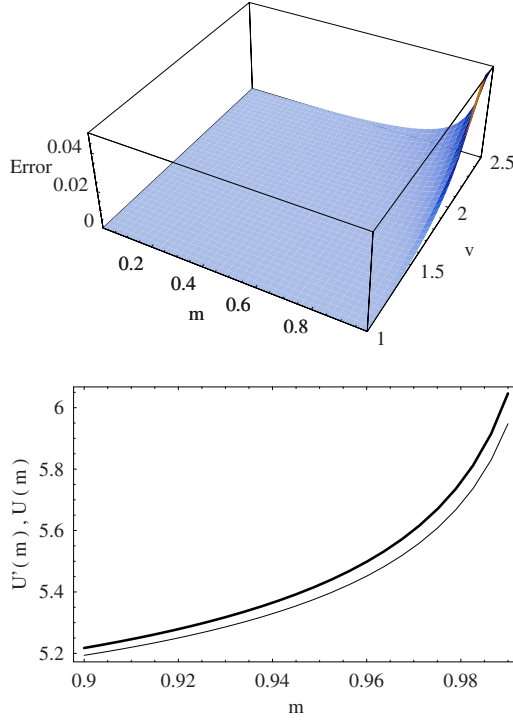
FIG. 4. (Color online) Top panel: Relative error $[U(m,v)$ $-\widetilde{U}(m,v)]/U(m,v)$ [cf. Eqs. (12) and (13)] for the parameters in the ranges $m \in [0,0.99]$ and $v \in [1,2.5]$. Bottom panel: Functions $U(m,v=2)$ (thick line) and $\widetilde{U}(m,v=2)$ (thin line) in the range $m \in [0.9,0.99]$. The quantities plotted are dimensionless.

otic threshold associated with the single-humped trigonometric optical lattice [cf. Eq. (14)]. It is worth noting that very similar quantitative predictions are obtained for a moving periodic optical lattice given by $V_0 cn^2(\kappa\xi;m)$, where $cn(\cdot;m)$ is the Jacobian elliptic cosine function of parameter m. Mathematically, this is because of the fundamental relationship $cn^2(\cdot;m)+sn^2(\cdot;m)=1$ together with the fact that the periodic lattice acts as a parametric excitation in Eq. (4) (and hence the Melnikov integral corresponding to the unity term of the fundamental relationship vanishes). Physically, one has indeed that in the limiting case $m=1$ the elliptic optical lattice $cn^2(\kappa\xi;m)$ vanishes except on a set of points of Lebesgue measure zero, i.e., one again recovers a case with no moving periodic lattice where chaotic dynamics is no longer possible.

We next compare the MM analytical predictions with numerical results (bifurcation diagrams), but with the added caveat that one cannot expect too good a quantitative agreement between the two kinds of findings because the MM is a perturbative method generally related to transient chaos, while bifurcation diagrams provide information solely concerning steady chaos. A typical example is shown in Fig. 6 where the particle number density $R^2 = |\varphi|^2 = |\psi|^2$ is plotted vs the shape parameter m for the experimental parameters [18] $m_a=23m_p$ with m_p the proton mass, $\lambda_0=589$ nm, $\gamma=0.05$, $\widetilde{V}_0=2$, and $v_L=3\times 10^{-2}$ m/s such that $v=2.03$ and $g=$ -0.75. Typically, the BEC traveling-wave steady state goes from a chaotic state which propagates in the direction of the motion of the optical lattice to a steady-state equilibrium
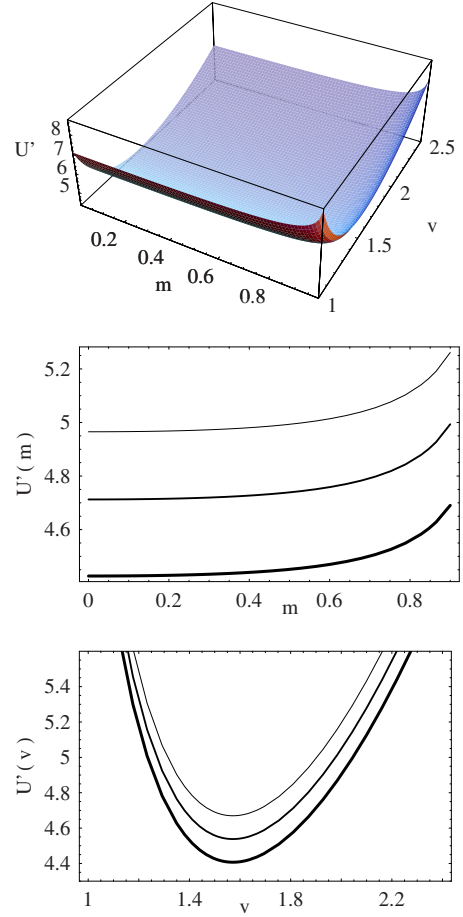

FIG. 5. (Color online) Plots of the chaotic threshold function $\widetilde{U}(m,v)$ [see Eqs. (13) and (14)]. Top panel: $\widetilde{U}$ vs m and v. Middle panel: $\widetilde{U}$ vs m for $v=1.5$ (thick line), 1.9 (medium line), and 2.03 (thin line). Bottom panel: $\widetilde{U}$ vs v for $m=0$ (thick line), 0.8 (medium line), and 0.9 (thin line). The quantities plotted are dimensionless.

associated with a static and uniform optical lattice as the shape parameter increases from 0 to 1. The progression of the steady states is characterized by the particle number density undergoing an inverse period-doubling route as the shape parameter is increased, which is preceded by diverse crises (see Fig. 6, bottom panel). We found similar regularization routes for other sets of experimentally realizable parameters, and would therefore emphasize that the present reshaping-induced control method could be implemented in experiments. Indeed, the two-term-approximation potential $p^{(2)}(\xi;m)=b_0 \sin^2(2\pi\xi/\lambda)+b_1 \sin^2(4\pi\xi/\lambda)$ [cf. Eq. (8)] used in the above theoretical analysis can be obtained from the two Fourier-synthesized counterpropagating laser beams

$$\mathbf{E}_1(\mathbf{r},t) = \frac{b_0^{1/2}(m)}{2} \mathrm{Re}(\varepsilon e^{-i(\omega t - kx + \pi/2)})$$

$$+ \frac{b_1^{1/2}(m)}{2} \mathrm{Re}(\varepsilon e^{-i(\omega t - 2kx + \pi/2)}),$$
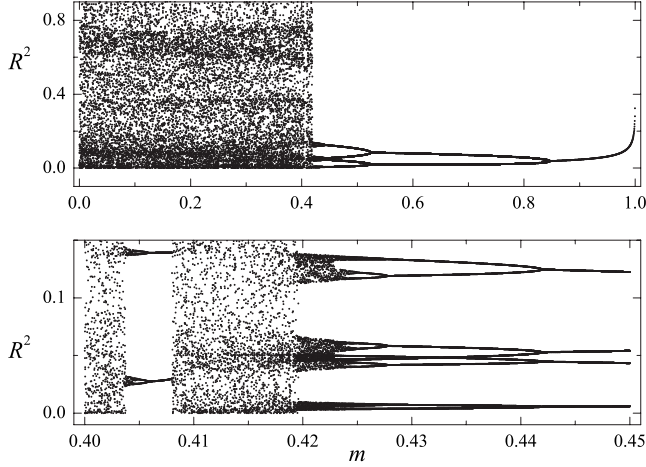
FIG. 6. Bifurcation diagrams of particle number density R^2 as a function of the shape parameter m for parameter values $\gamma = 0.05$, $\tilde{V}_0 = 2$, $v = 2.03$, and $g = -0.75$. Bottom panel shows the detail corresponding to the range where crises appear. The quantities plotted are dimensionless.

$$\mathbf{E}_2(\mathbf{r}, t) = \frac{b_0^{1/2}(m)}{2} \, \mathrm{Re}(\varepsilon e^{-i(\omega t + \delta t + kx - \pi/2)})$$
$$+ \frac{b_1^{1/2}(m)}{2} \, \mathrm{Re}(\varepsilon e^{-i(\omega t + 2\delta t + 2kx - \pi/2)}),$$

where ε is the common polarization [35].

III. SUMMARY

In summary, we have discussed a reshaping-induced method to suppress the existence of spatially chaotic steady-state traveling waves of a BEC with attractive interatomic interaction loaded into a traveling optical lattice of variable shape. We demonstrated theoretically and numerically that traveling spatially chaotic steady states of the particle number density can be reliably suppressed by small changes of the traveling optical lattice shape while keeping the remaining parameters constant. Finally, we provided an explicit expression for the two Fourier-synthesized counterpropagating laser beams for possible experimental realization of the control method.

APPENDIX: DERIVATION OF FORMULAS (6)

Using the Fourier expansion of $sn(\cdot; m)$ [31], one has

$$sn^2(\zeta; m) = \frac{4\pi^2}{mK^2(m)} \sum_{n=0}^{\infty} \sum_{l=0}^{\infty} a_n(m) a_l(m)$$
$$\times \sin\left(\frac{(2n+1)\pi\zeta}{2K(m)}\right) \sin\left(\frac{(2l+1)\pi\zeta}{2K(m)}\right), \quad \text{(A1)}$$

where $a_n(m) \equiv q^{n+1/2}(1 - q^{2n+1})^{-1}$ with $q = q(m) \equiv \exp[-\pi K(1-m)/K(m)]$ being the nome [31]. After applying the trigonometric relationships $2 \sin \alpha \sin \beta = \cos(\alpha - \beta) - \cos(\alpha + \beta)$ and $\cos \alpha = 1 - 2 \sin^2(\alpha/2)$ to Eq. (A1), one straightforwardly obtains Eq. (6) with

$$b_0 = \frac{4\pi^2}{mK^2(m)} \{a_0^2(m) - 2a_1(m)[a_0(m) + a_2(m)]$$
$$+ O[a_1(m)a_2(m)]\},$$

$$b_1 = \frac{4\pi^2}{mK^2(m)} \{2a_0(m)[a_1(m) - a_2(m)] + O[a_0(m)a_2(m)]\},$$

$$b_2 = \frac{4\pi^2}{mK^2(m)} \{a_1^2(m) + 2a_0(m)a_2(m) + O[a_0(m)a_2(m), a_1^2(m)]\}.$$

$$\text{(A2)}$$

Since $a_n(m) = \mathrm{csch}[(n+1/2)\pi K(1-m)/K(m)]/2$, one sees that $\lim_{n\to\infty} a_n(m) = 0$, $\forall m \in [0, 1[$. Thus, for the purposes of the present work, Eq. (A2) can be approximated by Eq. (7) and the remaining coefficients b_n with $n > 2$ are negligible over the range $0 \leq m \lesssim 0.99$.

[1] F. Dalfovo, S. Giorgini, L. P. Pitaevskii, and S. Stringari, Rev. Mod. Phys. **71**, 463 (1999).

[2] A. J. Leggett, Rev. Mod. Phys. **73**, 307 (2001).

[3] M. C. Gutzwiller, *Chaos in Classical and Quantum Mechanics* (Springer-Verlag, New York, 1990).

[4] *Emergent Nonlinear Phenomena in Bose-Einstein Condensates: Theory and Experiment*, edited by P. G. Kevrekidis, D. J. Frantzeskakis, and R. Carretero-González, Springer Series on Atomic, Optical, and Plasma Physics, Vol. 45 (Springer, Berlin, 2008).

[5] R. Carretero-González, D. J. Frantzeskakis, and P. G. Kevrekidis, Nonlinearity, **21**, R139 (2008).

[6] F. Kh. Abdullaev and R. A. Kraenkel, Phys. Rev. A **62**, 023613 (2000).

[7] C. Lee, W. Hai, L. Shi, X. Zhu, and K. Gao, Phys. Rev. A **64**, 053604 (2001).

[8] V. M. Eguiluz, E. Hernández-García, O. Piro, and S. Balle, Phys. Rev. E **60**, 6571 (1999).

[9] G. Chong, W. Hai, and Q. Xie, Phys. Rev. E **71**, 016202 (2005).

[10] A. D. Martin, C. S. Adams, and S. A. Gardiner, Phys. Rev. Lett. **98**, 020402 (2007).

[11] G. Chong, W. Hai, and Q. Xie, Phys. Rev. E **70**, 036213 (2004).

[12] V. S. Filho, A. Gammal, T. Frederico, and L. Tomio, Phys. Rev. A **62**, 033605 (2000).

[13] H. Saito and M. Ueda, Phys. Rev. Lett. **86**, 1406 (2001).

[14] P. Coullet and N. Vandenberghe, Phys. Rev. E **64**, 025202(R) (2001).

[15] T. Salger, C. Geckeler, S. Kling, and M. Weitz, Phys. Rev. Lett. **99**, 190405 (2007).

[16] P. A. Ruprecht, M. Edwards, K. Burnett, and C. W. Clark,

Phys. Rev. A **54**, 4178 (1996).

[17] P. Öhberg and S. Stenholm, J. Phys. B **32**, 1959 (1999).

[18] J. H. Denschlag, J. E. Simsarian, H. Häffner, C. McKenzie, A. Browaeys, D. Cho, K. Helmerson, S. L. Rolston, and W. D. Phillips, J. Phys. B **35**, 3095 (2002).

[19] I. Marino, S. Raghavan, S. Fantoni, S. R. Shenoy, and A. Smerzi, Phys. Rev. A **60**, 487 (1999).

[20] A. Aftalion, Q. Du, and Y. Pomeau, Phys. Rev. Lett. **91**, 090407 (2003).

[21] L. P. Pitaevskii, Sov. Phys. JETP **35**, 282 (1959).

[22] M. Tsubota, K. Kasamatsu, and M. Ueda, Phys. Rev. A **65**, 023603 (2002).

[23] K. Kasamatsu, M. Tsubota, and M. Ueda, Phys. Rev. A **67**, 033610 (2003).

[24] J. C. Bronski, L. D. Carr, B. Deconinck, and J. N. Kutz, Phys. Rev. Lett. **86**, 1402 (2001).

[25] L. D. Carr, J. N. Kutz, and W. P. Reinhardt, Phys. Rev. E **63**, 066604 (2001).

[26] J. C. Bronski, L. D. Carr, B. Deconinck, J. N. Kutz, and K. Promislow, Phys. Rev. E **63**, 036612 (2001).

[27] J. C. Bronski, L. D. Carr, R. Carretero-González, B. Deconinck, J. N. Kutz, and K. Promislow, Phys. Rev. E **64**, 056615 (2001).

[28] B. Deconinck, J. N. Kutz, M. S. Paterson, and B. W. Warner, J. Phys. A **36**, 5431 (2003).

[29] N. A. Kostov, V. Z. Enolskii, V. S. Gerdjikov, V. V. Konotop, and M. Salerno, Phys. Rev. E **70**, 056617 (2004).

[30] V. S. Gerdjikov, B. B. Baizakov, M. Salerno, and N. A. Kostov, Phys. Rev. E **73**, 046606 (2006).

[31] See, e.g., L. M. Milne-Thomson, in *Handbook of Mathematical Functions*, edited by M. Abramowitz and I. A. Stegun (Dover, New York, 1972).

[32] See, e.g., J. Guckenheimer and P. J. Holmes, *Nonlinear Oscillations, Dynamical Systems, and Bifurcations of Vector Fields* (Springer, Berlin, 1983).

[33] V. K. Melnikov, Trans. Mosc. Math. Soc. **12**, 1 (1963).

[34] An explicit expression for $U(m,v)$ is available by using MATHEMATICA but its size and algebraic complexity prevent us from showing it easily.

[35] G. Grynberg and C. Robilliard, Phys. Rep. **355**, 335 (2001).

[36] Note that more complicated $\theta(\zeta)$ dependences are also possible; however, they are likely to yield a system of differential equations for the amplitude [the equivalent of Eq. (4)] that cannot be analytically tractable using Melnikov's method.